

## Accepted Manuscript

Title: Fate and impact of organics in an immersed membrane bioreactor applied to brine denitrification and ion exchange regeneration

Authors: Ewan J. McAdam, Mark Pawlett, Simon J. Judd

PII: S0043-1354(09)00564-8

DOI: [10.1016/j.watres.2009.08.048](https://doi.org/10.1016/j.watres.2009.08.048)

Reference: WR 7610

To appear in: *Water Research*

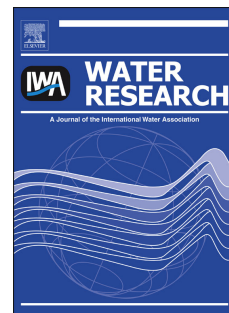
Received Date: 18 March 2009

Revised Date: 17 August 2009

Accepted Date: 30 August 2009

Please cite this article as: McAdam, E.J., Pawlett, M., Judd, S.J. Fate and impact of organics in an immersed membrane bioreactor applied to brine denitrification and ion exchange regeneration, *Water Research* (2009), doi: [10.1016/j.watres.2009.08.048](https://doi.org/10.1016/j.watres.2009.08.048)

This is a PDF file of an unedited manuscript that has been accepted for publication. As a service to our customers we are providing this early version of the manuscript. The manuscript will undergo copyediting, typesetting, and review of the resulting proof before it is published in its final form. Please note that during the production process errors may be discovered which could affect the content, and all legal disclaimers that apply to the journal pertain.



1 **Fate and impact of organics in an immersed membrane bioreactor applied to**  
2 **brine denitrification and ion exchange regeneration**

3 *Ewan J. McAdam<sup>1</sup>, Mark Pawlett<sup>2</sup>, Simon J. Judd<sup>1</sup>*

4 <sup>1</sup>*Centre for Water Science, Cranfield University, Bedfordshire, MK43 0AL*

5 <sup>2</sup>*Natural Resources Department, Cranfield University, Bedfordshire, MK43 0AL*

6

7 **ABSTRACT**

8 The application of membrane bioreactors (MBRs) to brine denitrification for ion  
9 exchange regeneration has been studied. The developed culture was capable of  
10 complete brine denitrification at 50 gNaCl.l<sup>-1</sup>. Denitrification reduced to c.60% and  
11 c.70% when salinity was respectively increased to 75 and 100 g.l<sup>-1</sup>, presumed to be  
12 due to reduced growth rate and the low imposed solids retention time (10 days).  
13 Polysaccharide secretion was not induced by stressed cells following salt shocking,  
14 implying that cell lysis did not occur. Fouling propensity, monitored by critical flux,  
15 was steady at 12-15 l.m<sup>-2</sup>.h<sup>-1</sup> during salinity shocking and after brine recirculation,  
16 indicating that the system was stable following perturbation. Low molecular weight  
17 polysaccharide physically adsorbed onto the nitrate selective anion exchange resin  
18 during regeneration reducing exchange capacity by c.6.5% when operating up to  
19 complete exhaustion. However, based on a breakthrough threshold of 10 mgNO<sub>3</sub><sup>-</sup>-N.l<sup>-1</sup>  
20 <sup>1</sup> the exchange capacity was comparative to that determined when using freshly  
21 produced brine for regeneration. It was concluded that a denitrification MBR was an  
22 appropriate technology for IEX spent brine recovery and reuse.

23

24 **Keywords:** *Ion-exchange; brine; biological denitrification; salt; nitrate*

25

26

## 27 1. INTRODUCTION

28 Anion-exchange (aIEX) is the most frequently adopted technology for nitrate ( $\text{NO}_3^-$ )  
29 removal during potable water treatment due to its low cost and operational simplicity.  
30 A strong salt (NaCl) solution is used to regenerate the resin resulting in the production  
31 of concentrated waste brine containing the target anion, chloride and other oxyanions.  
32 This waste stream can comprise 0.8 to 2.4% of treated product flow (McAdam and  
33 Judd, 2008) and its disposal (usually by tankering) constitutes a significant proportion  
34 of the process cost. Operation of aIEX in combination with biological nitrate  
35 reduction of the waste brine for regenerant recovery presents a more sustainable  
36 alternative by reducing the waste volume, salt (NaCl) consumption and treated  
37 product losses.

38  
39 Studies adapting non-halophilic microbial communities from standard activated  
40 sludge processes for this application have reported inhibition of denitrification and, in  
41 some cases, plasmolysis to be promoted by the elevated salt concentrations  
42 ( $>30\text{gNaCl.l}^{-1}$ ). More recently, halophilic monocultures *Halomonas denitrificans*  
43 (Cyplik et al., 2007) and *Halomonas campisalis* (Peyton et al., 2001) have been  
44 successfully adapted at laboratory scale for denitrification at high salt concentrations  
45 from 30 to 180  $\text{g.l}^{-1}$ , obviating dilution prior to biotreatment. However, adaptation of  
46 halophiles to brine processing is yet to be examined in detail.

47  
48 Other restrictions to this application include the accumulation of inorganic  
49 constituents (e.g. sulphate) due to recirculation, and the impact of organics and  
50 microbial carryover from the bioreactor on downstream resin regeneration. In brine  
51 re-use trials, elevated sulphate concentrations were not reported to impact upon either

52 resin or biological performance when nitrate selective resins have been used (Clifford  
53 and Liu, 1993). However, Bae et al. (2002) reported that microbial associated  
54 particulates and organics present in the regenerant fouled anion exchange resins, thus  
55 the integration of both sand filtration and GAC were required downstream of the  
56 denitrification reactor to nullify the impact. Though little information exists on the  
57 impact of residual organics on resin capacity, the application of “classical” biomass  
58 separation membrane bioreactor (MBR) technology to this duty has been mooted to  
59 provide absolute bacterial rejection and high MW biopolymer retention, promoting a  
60 consistent permeate quality (McAdam and Judd, 2008).

61

62 The current paper assesses the viability of a denitrification MBR for waste aIEX brine  
63 treatment and reuse in the regeneration of ion exchange resins, specifically this study  
64 will address: the fate of organics during permeate brine recirculation (to simulate re-  
65 use); the impact of organics on resin capacity; the influence of salt variation on  
66 halophilic treatment performance; and the impact of perturbation on fouling  
67 propensity.

68

## 69 **2. MATERIAL AND METHODS**

### 70 **2.1 Experimental rig**

71 To establish a salt tolerant bacterial community, a seed culture was harvested from the  
72 anaerobic layer of a coastal sediment at low tide. Following acclimation in batch  
73 conditions ( $50 \text{ gNaCl.l}^{-1}$ ,  $500 \text{ mgNO}_3^- \text{-N.l}^{-1}$ ), a 75 l reactor (Figure 1) was seeded at a  
74 v/v ratio of 15:1. The influent nitrate concentration was set at  $500 \text{ mg NO}_3^- \text{-N.l}^{-1}$ .  
75 During substrate optimisation, ethanol was supplied as the exogenous substrate and  
76 dosed at a C:N ratio of between 0.77:1 and 8.5:1 ( $\text{g.g}^{-1}$ ); under normal conditions, a

77 C:N of 0.85:1 was used. Reactor temperature was maintained at c.20°C using a  
78 thermostatically controlled heating jacket. An impeller mixer was used to ensure  
79 complete biomass distribution with the impeller blade sited below the membrane  
80 module. The hydraulic and solids residence times (HRT and SRT respectively) were  
81 17.5 hours and 10 days respectively. The process was allowed 3 SRTs to acclimatise  
82 prior to testing. During recirculation experiments, MBR permeate was collected in a  
83 holding tank ( $T_2$ ), supplemented with  $\text{NO}_3^-$  and pumped back to the feed tank ( $T_1$ ).  
84 During salt upshocking/ downshocking experiments, the NaCl concentrate dosed into  
85  $T_1$  was changed to meet the required concentration providing an incremental spike;  
86 fluid residence time in  $T_1$  was approximately 20 hours.

87

88 A 0.93 m<sup>2</sup> out-to-in immersed PVDF hollow-fibre membrane with 0.04 µm nominal  
89 pore size was used. Permeate was withdrawn under suction from the membrane using  
90 a piston pump (FMI Inc., Syosset, US). To maintain anoxic conditions, nitrogen-  
91 enriched air (>99%) was used to scour the membrane. Gas was introduced via a  
92 solenoid valve (Zoedale Plc, Bedford, UK) and controlled with a programmable  
93 digital relay (Kübler GmbH, Ludwigshafen, Germany); flow rate was controlled with  
94 a 0-50 l min<sup>-1</sup> needle valve (RS Ltd., Corby, UK). Pressure was monitored using a -  
95 0.5 to 0.5 barg calibrated pressure transducer (Gem Sensors, Basingstoke, UK) and  
96 data recorded using a 16-bit 0 to 2.5 V data conversion unit (Pico technology, St.  
97 Neots, UK).

98

## 99 **2.2 Anion exchange resin**

100 A commercially available nitrate selective macroporous styrene based anion exchange  
101 resin (Purolite A520E, Llantrisant, UK) was loaded into a 50mm diameter x 1m glass

102 chromatography column and retained using 25  $\mu\text{m}$ -rated frits at either end; the bed  
103 comprised 120g of resin. After initial rinsing, the A520E resin size ranged from 0.28  
104 to 1.26 mm ( $d_{50}$  0.61 mm). Prior to use, DI water was pumped through the resin bed  
105 at 20 bed volumes (Bv).h<sup>-1</sup> for 30 minutes, followed by a 30 minute 50gNaCl.l<sup>-1</sup> flush  
106 (to ensure saturation) at 5 Bv.h<sup>-1</sup> and a subsequent DI rinse for 60 minutes at 5 Bv.h<sup>-1</sup>.  
107 The exhaustion flow rate was set to 20 Bv.h<sup>-1</sup> and the IEX feed contained 30 mgSO<sub>4</sub><sup>2-</sup>  
108 .l<sup>-1</sup>, 115 mgCl.l<sup>-1</sup>, 150 mgCaCO<sub>3</sub>.l<sup>-1</sup> and 22.6 mg.l<sup>-1</sup> NO<sub>3</sub><sup>-</sup>-N. Regeneration comprised  
109 a 60 minute cycle at 5 Bv.h<sup>-1</sup> followed by slow and fast rinses of 5 Bv.h<sup>-1</sup> for 30  
110 minutes and 20 Bv.h<sup>-1</sup> for 10 minutes respectively.

111

## 112 **2.3 Chemical analysis**

### 113 *2.3.1 General analysis*

114 Mixed liquor suspended solids (MLSS) and bicarbonate were determined by standard  
115 methods. Oxyanion (NO<sub>3</sub><sup>-</sup>, NO<sub>2</sub><sup>-</sup>) and chloride concentration was measured using  
116 proprietary cell tests (Merck Spectroquant) with spectrophotometric detection.  
117 Dissolved organic carbon (DOC) was measured using a Shimadzu TOC-5000A  
118 analyser. Ethanol concentration was determined using a commercially available  
119 enzymatic method (Boehringer-Mannheim, Roche). Soluble microbial products  
120 (SMP) were extracted according to the method described in Judd (2006) and  
121 polysaccharide and protein concentration quantified using the phenol–sulphuric acid  
122 method (Zhang et al., 1999) and modified Lowry method (Frølund et al., 1995)  
123 respectively. Absorbance for polysaccharide and protein determinations was  
124 measured using a Jenway 6505 UV/Vis spectrophotometer at UV<sub>480nm</sub> and UV<sub>750nm</sub>  
125 respectively with D-glucose and bovine serum albumin (BSA) as standards. Particle

126 size distribution was measured with an integrated laser diffractor (Malvern  
127 Mastersizer 2000).

128

### 129 2.3.2 *Molecular weight fractionation*

130 Serial fractionation was undertaken using an Amicon 8400 series stirred cell,  
131 pressurised with N<sub>2</sub> (1 barg), and standard UF (Millipore) membranes, size range 10,  
132 30, 50, 100 and 300kDa. Sample supernatant was pre-filtered using a 1.2µm filter and  
133 the subsequent sample split between two 300 kDa membranes to limit concentration  
134 polarisation. Concentration polarisation was limited by application of an integrated  
135 bar stirrer operate at a constant 100 rpm; the adopted filtrate/ retentate ratio was 0.4.

136

### 137 2.3.3 *Phospholipid fatty acid analysis*

138 Phospholipid fatty acid (PLFA) analysis was used to assess the community structure  
139 using the method of Frostegård et al. (1991). Samples were freeze dried prior to  
140 analysis. Lipids were extracted from the freeze dried sample using the Bligh and Dyer  
141 (1959) ratio of 1:2:0.8 (v/v/v) of chloroform, methanol and citrate buffer. Lipids were  
142 then fractionated by solid phase extraction. The phospholipid fraction was derivatised  
143 by mild alkaline methanolysis (Dowling et al., 1986). The resultant fatty-acid methyl  
144 esters (FAMES) were analyzed by GC-FID (Agilent). Peak identification was  
145 undertaken using GC-MS (Agilent).

146

## 147 **3. RESULTS**

### 148 **3.1 Exogenous and endogenous organics transmission at steady state**

149 Nitrate removal efficiency increased from 84.6% to a maximum 99.8% as the carbon  
150 to nitrogen ratio (C:N) increased from 0.77 to 0.94 (Figure 2). Once a C:N ratio of

151 0.89 had been exceeded, ethanol was detected in the permeate above the limit of  
152 detection ( $>0.5 \text{ mg l}^{-1}$ ). Although the existence of an optimum C:N has been reported  
153 previously (McAdam et al., 2007), research studies typically observe low  $\text{NO}_2^-$ -N and  
154  $\text{NO}_3^-$ -N effluent concentrations as the optimum C:N is exceeded due to the surplus of  
155 available carbon (Chiu and Chung, 2003; McAdam et al., 2007). In this study, on  
156 increasing C:N  $>0.98$  inhibition was observed resulting in 71-97% of the available  
157  $\text{NO}_3^-$  being converted to  $\text{NO}_2^-$  for C:N values up to 8.5. Yoshie et al. (2006) also  
158 reported nitrite accumulation in concentrated brines indicating reductase activity  
159 maybe very different at high salinity.

160

161 Protein and polysaccharide transmission through the membrane at steady state were  
162  $27.3\% \pm 8.0\%$  and  $81.5\% \pm 10.5\%$  respectively. Fawehinmi (2006) observed similar  
163 transmission rates for proteins and polysaccharides, recording 49% and 80%  
164 respectively, for operation of an anaerobic immersed hollow fibre ( $0.1 \mu\text{m}$ ) MBR. In  
165 this study, SMP exhibited a principal protein peak of 55.1% between  $<1.2 \mu\text{m}$  and  
166 300 kDa and a principal polysaccharide peak of 48.3% below 10 kDa (Figure 3).  
167 Organics between  $1.2 \mu\text{m}$  and 100 kDa were absent in the permeate indicating the  
168 molecular weight cut off (MWCO) of the hollow-fibre (and any associated biofilm)  
169 was c.50 to 100 kDa.

170

### 171 **3.2 Impact of organics accumulation during recirculation**

172 After 7 days recirculation, the SMP DOC had increased from an initial concentration  
173 of c. $170 \text{ mgDOC.l}^{-1}$  (c. $34 \text{ mgDOC.gMLSS}^{-1}$ ) up to a maximum concentration of 557  
174  $\text{mgDOC.l}^{-1}$  (Figure 4). At steady state, DOC transmission was recorded between 54%



175 and 80% and was attributed to accumulation of low molecular weight (MW) organics  
176 (below the membrane MWCO).

177

178 Critical flux analysis ( $J_c$ ) was conducted using the flux step method before  
179 recirculation and after reaching steady state (Figure 5). In both cases,  $J_c$  was between  
180 12 and 15  $\text{l.m}^{-2}.\text{h}^{-1}$ . Interestingly, similar exponential  $dP/dt$  trends were obtained for  
181 both sets of conditions, evidenced by similar gradients ( $(dP/dt)/J$ ) of between 0.23 and  
182 0.27, however,  $dP/dt$  measured post-recirculation exhibited lower overall fouling  
183 potential. This appears counter-intuitive, based on the presence of accumulated  
184 organics and challenges previous reports which link fouling propensity to elevated  
185 concentrations of biopolymers in the bulk phase (Judd, 2006; Reid et al., 2006).

186

### 187 **3.3 IEX Resin capacity**

188 To allow comparison with previous aIEX resin studies (Clifford and Liu, 1993; Bae et  
189 al., 2002),  $\text{NO}_3^-$ -N breakthrough curves were determined using a  $10 \text{ mgN.l}^{-1}$  threshold  
190 effluent concentration (US regulatory limit). Breakthrough curves (1 to 6) were run to  
191 complete exhaustion initially using freshly produced regenerant ( $\text{Brine}_{\text{fp}}$ ,  $50\text{gNaCl.l}^{-1}$ ,  
192 Figure 6(a)). The threshold was reached at c.400 bed volumes (BVs) in the second run  
193 which corresponded to a resin capacity of  $0.61 \text{ eq.l}^{-1}$  or 88% of throughput obtained  
194 with the virgin resin during the first run. Subsequent runs 3 to 6 indicated a near  
195 identical trend demonstrating reproducible regeneration efficiency under these  
196 conditions. A capacity of c. $0.46 \text{ eq.l}^{-1}$  has been observed previously by Bae et al.  
197 (2002) using the same commercially available resin (A520E); the lower capacity may  
198 be explained by the authors' application of a lower strength regenerant ( $30\text{gNaCl.l}^{-1}$ ).

199

200 Breakthrough curves (1-6) were subsequently generated with fresh resin using  
201 biologically treated brine ( $\text{Brine}_{\text{bt}}$ ,  $50\text{gNaCl.l}^{-1}$ ) as the regenerant (Figure 6(b)).  
202  $\text{Brine}_{\text{bt}}$  was sampled from the MBR permeate once steady state had been reached  
203 during permeate recirculation. At steady state, the DOC concentration of the  $\text{brine}_{\text{bt}}$   
204 was c.287  $\text{mg.l}^{-1}$ . Under these conditions, breakthrough occurred at c.390 BVs in the  
205 second run, corresponding to 0.58  $\text{eq.l}^{-1}$  or 87% of throughput obtained with the virgin  
206 resin during the first run. Comparison with Run 4 (a) using  $\text{brine}_{\text{fp}}$  (Figure 6(b))  
207 demonstrated a loss in capacity (Area 1) indicating the extent of interference created  
208 by the biologically derived organics. Integration of the area between the  $\text{brine}_{\text{fp}}$  and  
209  $\text{brine}_{\text{bt}}$  exhaustion curves recorded a capacity loss of 59  $\text{meq.l}^{-1}$  or c.6.5% of the  
210 estimated exhaustive resin capacity. Bae et al. (2002) observed significant capacity  
211 losses when using permeate from an upflow sludge blanket reactor (USBR) for  
212 regeneration unless subsequent treatment steps were incorporated. However, in this  
213 study subsequent regenerations using  $\text{brine}_{\text{bt}}$  displayed a similar reproducibility  
214 indicating that the resin had reached a maximum organic capacity at the end of the  
215 first regeneration cycle.

216

217 The uptake of  $\text{brine}_{\text{bt}}$  organics by the resin was quantified using a virgin salt saturated  
218 resin (Figure 7). Brine regenerant was assumed to exit the column once chloride  
219 transmission reached 100% (assuming chloride uptake to be zero at saturation).  
220 Chloride and protein transmission reached 100% simultaneously between 1 and 1.5  
221 BVs indicating protein adsorption to be negligible. Polysaccharide and DOC  
222 transmission were recorded at c.15% and c.90% respectively up to 4 BVs, where a  
223 rapid increase in transmission in the interval between 4 and 7 BVs was observed. At 7  
224 BVs, polysaccharide and DOC transmission reached 100%, indicating saturation of

225 the resin with polysaccharide. Total adsorbed DOC on the 120g resin bed was  
226 estimated at 26.4 mg (0.22 mgDOC.gResin). During exhaustion/regeneration cycles  
227 (Figure 6(b)), the adsorptive mechanism of the polysaccharides was evaluated by  
228 regenerating the resin with a 50/50 fresh brine/biological regenerant (Run 5) and  
229 100% fresh brine (Run 6). The similarity of the subsequent exhaustion curves  
230 suggested low polysaccharide exchange potential (i.e. reversibility).

231

### 232 **3.4 Salt shocking**

233 To reflect the significant salt variations occurring in brine regenerant waste, the  
234 regenerant was initially upshocked to 75 gNaCl.l<sup>-1</sup> which was subsequently further  
235 increased to 100 gNaCl.l<sup>-1</sup> after 7 days. Following the initial upshock (75 gNaCl l<sup>-1</sup>),  
236 nitrate removal decreased from 99.7 to 60.1% (Table 1) demonstrating a decrease in  
237 the specific biomass denitrification capacity. Protein release was also recorded with  
238 an increase in bulk phase concentration from c.30 to c.50 mg.l<sup>-1</sup> and from c.15 to c.30  
239 mg.l<sup>-1</sup> following salt upshock to 75 and 100 gNaCl.l<sup>-1</sup> respectively (Figure 8). A  
240 transition in floc structure also occurred; at steady state (50 gNaCl.l<sup>-1</sup>), a floc size  
241 distribution ranging 60 to 800µm was measured, however, following upshocking to  
242 75 gNaCl.l<sup>-1</sup>, a bi-modal distribution was recorded with the dominant peak ranging  
243 0.2 to 5µm, indicating floc breakage into primary particles (Wilén et al., 2003). After  
244 7 days at 100gNaCl.l<sup>-1</sup>, the system was downshocked to 50 gNaCl.l<sup>-1</sup>; sampling 24  
245 hours after downshocking demonstrated near complete denitrification recovery to  
246 98.4%.

247

248 Although the volume of particulate and colloidal material had apparently increased,  
249 critical flux analysis conducted before and after each salt increment (Figure 9)

250 indicated that fouling propensity remained stable as demonstrated by the similar  $dP/dt$   
251 trends obtained. In addition,  $J_c$  was consistently recorded at c.12  $\text{l.m}^{-2}.\text{h}^{-1}$  and is  
252 comparable to that recorded during steady-state recirculation. This contradicts a  
253 previous non-halophilic MBR study where upon exposure to a  $5 \text{ g.l}^{-1}$  chloride residual  
254 (0.83% NaCl) both protein and polysaccharide were released causing permeability  
255 decline (flat sheet,  $0.4 \mu\text{m}$ ) which was correlated to the elevated SMP polysaccharide  
256 concentration (Reid et al., 2006); the absence of elevated concentrations of secreted  
257 polysaccharide in this current study may in part explain this disparity.

258

259 Twenty PLFA fatty acid methyl esters (FAMES), identified by MS, principally  
260 comprised normal saturates and terminally branched saturates. Trans-monoenoic fatty  
261 acid concentrations were below the limit of detection. Dominant FAMES were C16:0,  
262 C16:1, C17:0, C18, C18:1 $\omega$ 9c and C19:0cy at 50, 75 and  $100 \text{ gNaCl.l}^{-1}$  and accounted  
263 for c.95% of PLFAs detected (Table 2). Similar elution profiles (and the absence of  
264 trans-monoenoic fatty acids) were observed previously for a range of moderately and  
265 extremely halophilic bacterium (Aston and Peyton, 2007; Yakimov et al., 2001).  
266 Principal component analysis (PCA) showed three discrete data groupings  
267 corresponding to salt concentration (Figure 10). Analysis of variance of the principal  
268 components (PC) confirmed significant differences of  $P<0.001$  and  $P<0.01$  for  
269 principal components PC1 and PC2 respectively. This distinction indicates abrupt  
270 changes in phenotypic profile between step changes in salinity.

271

## 272 **4. DISCUSSION**

### 273 **4.1 MBR Fouling**

274 High polysaccharide transmission of c.81.5% was observed during steady state due to  
275 the production of low MW biopolymers and corresponded to a mean DOC removal of  
276 c.44%. Low MW biopolymers are generally associated with substrate metabolism and  
277 biomass growth (Barker et al., 2000) and are produced in all MBR applications. Using  
278 LC-OCD, Zhang et al. (2006) observed 99.8% high MW (c.250 kDa) and 93.6% low  
279 MW (5 to 250 kDa) biopolymer rejection when using a 0.2  $\mu\text{m}$  flat sheet membrane in  
280 an MBR and cited polysaccharide as the major foulant. The authors suggested this  
281 behaviour to be a common trait of fouled MF membranes; improved retention of low  
282 MW biopolymers (and higher  $dP/dt$ ) in their investigation may arise from more  
283 significant internal deposition created by the larger pore size. In this study,  
284 concentration (accumulation) of low MW biopolymers in the bulk phase by permeate  
285 recirculation did not increase fouling propensity. This indicates that: (1) low MW  
286 biopolymers asserted poor aggregation potential upon recirculation and thus were not  
287 filtered; and (2) biopolymers exhibited limited binding potential to the membrane  
288 surface and any biofilm present. This contradicts previous experiences with  
289 polysaccharides (Zhang et al., 2006; Frank and Belfort, 2003), however, past research  
290 has typically focused on high MW polysaccharides (100 to 1600 kDa) which possess  
291 more structural and functional complexity than those of lower MW biopolymers  
292 (48.3% below 10 kDa) as in this study; higher MW structures may thus concentrate at  
293 the membrane surface by both size exclusion and surface adhesion (Frank and Belfort,  
294 2003).

295

296 Fouling propensity was not greatly increased by salt shocking. The characteristic  
297 response of non-halophilic micro-organisms exposed to salt upshock is to undergo  
298 plasmolysis due to a loss in turgor pressure (Reid et al., 2006). This induces the

299 release of soluble cellular components through the cell membrane (Lapidou and  
300 Rittmann, 2002) and in some instances the subsequent release of cell wall components  
301 such as acid mucopolysaccharides, resulting in high concentrations of proteins and  
302 polysaccharides in the bulk phase (Reid et al., 2006, Zhang et al., 2006). In this study,  
303 only protein was released, implying that cell lysis did not occur. Halophilic bacteria  
304 possess modified highly negatively charged proteins on the external cell wall to  
305 mediate osmotic shifts (Petrovic et al., 1999); the protein release observed may  
306 therefore have been an adjustment in cell wall composition (Russell, 1989). In  
307 addition, cell wall modification may have initiated the floc destabilisation observed  
308 upon upshocking causing indirect release of extracellular protein from the floc matrix  
309 as postulated by Reid et al. (2006). The absence of secreted polysaccharide, structure  
310 and size distribution of the organics produced by halophilic bacteria and the lower  
311 membrane pore size adopted in this investigation (0.04  $\mu\text{m}$ , potentially limiting  
312 internal deposition) may explain the disparity in organics rejection and fouling  
313 compared to previous literature findings (Reid et al., 2006; Zhang et al., 2006).

314

#### 315 **4.2 Microbial community and treatment performance**

316 PLFA profiles were dominated by a small range of fatty acids that are common  
317 amongst halophiles (Aston and Peyton, 2007; Yakimov et al., 2001). The trans/cis  
318 ratio was consistently  $<0.15$  at all three salt concentrations indicating that the cell  
319 membrane remained stable - a ratio above 0.25 indicating instability (Aston and  
320 Peyton, 2007) - further suggesting that plasmolysis did not occur. Transition of PLFA  
321 profiles at each salt increment indicated reordering of the membrane lipid  
322 composition for osmoregulation (Russell, 1989; Pflüger and Muller, 2004) and  
323 microbial community restructuring (Forney et al., 2001) as described previously for

324 salt upshocking of denitrifying halophiles (Yoshie et al., 2006). The decrease in  
325 nitrate removal from 99.7% to between 58.6% and 73.6% may therefore be due to  
326 microbial restructuring, however, lower specific bacterial growth rates have been  
327 observed at high salt concentrations. Peyton et al. (2001) established that *Halomonas*  
328 *campisalis* could effectively denitrify at 180 gNaCl.l<sup>-1</sup> (Peyton et al., 2001), though  
329 the maximum specific growth rate for the monoculture was identified at c.30gNaCl.l<sup>-1</sup>  
330 (Aston and Peyton, 2007). In this study, upon down shocking to 50gNaCl.l<sup>-1</sup>  
331 denitrification capacity recovered to 98.4% within 24 hours. This demonstrates that  
332 whilst transition in community structure occurred following salt upshocking, an  
333 effective residual halotolerant denitrifying community remained following  
334 perturbation; extension of SRT (>10 days) may be sufficient to offset the lower  
335 growth rates observed at high salt concentrations.

336

### 337 **4.3 Resin operation**

338 It has been suggested that polysaccharides do not normally deposit easily onto aIEX  
339 resin due to impeded diffusion (by size exclusion) and low contact times (Cornelissen  
340 et al., 2008). In this study, polysaccharides contacted the resin during regeneration  
341 rather than exhaustion, thus increasing contact time by a factor of four. Adsorption of  
342 exopolysaccharides to anionic resins is intuitive as their structure is principally  
343 polyanionic due to the number of uronic acid or ketal linked pyruvate groups  
344 contained within the long chain high MW (500-2000 kDa) structures (Sutherland,  
345 2001). However, based on the low affinity shown for desorption of polysaccharides in  
346 this study, it appears that the dominant adsorption mechanism associated with the  
347 lower MW polysaccharides present in the brine is physical rather than exchange  
348 based. DOC uptake could not be quantified during exhaustion runs due to competition

349 effects with the influent DOC. Therefore, based on physical data, the theoretical  
350 charge density (approximated by normalising lost resin capacity with DOC uptake,  
351 Figure 7) was  $c.3.9 \times 10^{-4} \text{ meq.gDOC}^{-1}$ ; this negligible result further demonstrates that  
352 adsorption was not exchange based and indicates that the adsorbed organics exhibited  
353 a charge closer to neutrality. Kim and Symons (1991) postulated that physical  
354 adsorption was more likely to occur at the resin skeleton. After the first regeneration  
355 with brine<sub>bt</sub>, physical adsorption reached a maximum, presumably due to the limited  
356 number of adsorption sites available.

357

## 358 5. CONCLUSIONS

359 A study of the denitrification of high salinity ion exchange brine regenerant and the  
360 impact of accumulation on process performance has demonstrated recycling for ion  
361 exchange regeneration to be viable.

- 362 1. Whilst recirculation generated high concentrations of low MW organics, their  
363 impact on membrane permeability was negligible.
- 364 2. Although salt upshock induced protein release, the permeability decline was  
365 minimal, contrary to previous studies based on non-halophilic communities.
- 366 3. Nitrate removal of c.99.7% was observed at steady-state ( $50 \text{ gNaCl.l}^{-1}$ ); at salt  
367 concentrations above  $50 \text{ gNaCl.l}^{-1}$  nitrate removal decreased and the  
368 community profile was modified, though this could be countered by adoption  
369 of a higher SRT to offset the lower growth rates.
- 370 4. Adsorption of the low MW organics generated during denitrification onto the  
371 resin structure resulted in minimal loss in resin capacity, implying long-term  
372 operation using recovered brine is possible.



- 373 5. Under halophilic conditions, addition of exogenous substrate must be  
374 controlled to minimise breakthrough and to support complete denitrification  
375 (limiting the preferential formation of nitrite).
- 376 6. The efficacy of the denitrification MBR process is closely related to  
377 membrane rejection and the structural and functional attributes of the resultant  
378 organics; both the process operational determinants and the bacterial  
379 community generated may influence performance.

380

### 381 **Acknowledgements**

382 The authors would like to thank the Engineering and Physical Sciences Research  
383 Council (EPSRC), Anglian Water, Severn Trent Water and Yorkshire Water for their  
384 financial support.

385

### 386 **REFERENCES**

- 387 Aston, J.E., Peyton, B.M. (2007). Response of *Halomonas campisalis* to saline stress:  
388 changes in growth kinetics, compatible solute production and membrane phospholipid  
389 fatty acid composition. *FEMS Microbiol. Lett.* 274, 196-203.
- 390 Bae, B.-U., Jung, Y.-H., Han, W.-W., Shin, H.-S. (2002). Improved brine recycling  
391 during nitrate removal using ion exchange. *Water Res.* 36, 3330-3340.
- 392 Barker, D.J., Salvi, S.M.L., Langenhoff, A.A.M., Stuckey, D.C. (2000). Soluble  
393 microbial products in ABR treating low-strength wastewater. *J. Environ. Eng.* 126,  
394 239-249.
- 395 Bligh, E. G., Dyer, W. J. (1959). A rapid method of total lipid extraction and  
396 purification. *Can. J. Biochem. Physiol.* 37, 911-917.

- 397 Chiu, Y.-C., Chung, M.-S. (2003). Determination of optimal COD/nitrate ratio for  
398 biological denitrification. *International biodeterioration biodegradation*. 51, 43-49.
- 399 Clifford, D., Liu, X. (1993). Ion exchange for nitrate removal. *J. Am. Water Works*  
400 *Assoc.* 85, 135-143.
- 401 Cornelissen, E.R., Moreau, N., Siegers, W.G., Abrahamse, A.J., Rietveld, L.C.,  
402 Grefte, A., Dignum, M., Amy, G., Wessels, L.P. (2008). Selection of anionic  
403 exchange resins for removal of natural organic matter (NOM) fractions. *Water Res.*  
404 42, 413-423.
- 405 Cyplik, P., Grajek, W., Marecik, R., Króliczak, P., Dembczyński, R. (2007).  
406 Application of a membrane bioreactor to denitrification of brine. *Desalination*. 207,  
407 134-143.
- 408 Dowling, N. J. E., Widdel, F., White, D. C. (1986). Phospholipid ester-linked fatty  
409 acid biomarkers of acetate-oxidising sulphate-reducers and other sulphide-forming  
410 bacteria. *J. Gen. Microbiol.* 132, 1815-1825.
- 411 Fawehinmi, F. (2006). Anaerobic MBR treatment of a low strength municipal  
412 wastewater. PhD Thesis, Cranfield University, UK.
- 413 Forney, L.J., Liu, W.-T., Guckert, J.B., Kumagai, Y., Namkung, E., Nishihara, T.,  
414 Larson, R.J. (2001). Structure of microbial communities in activated sludge: Potential  
415 implications for assessing the biodegradability of chemicals. *Ecotoxicol. Environ. Saf.*  
416 49, 40-53.
- 417 Frank, B.P., Belfort, G. (2003). Polysaccharides and sticky membrane surfaces:  
418 critical ionic effects. *J. Membr. Sci.* 212, 205-212.
- 419 Frølund, B., Griebe, T., Nielsen, P.H. (1995). Enzymatic activity in the activated-  
420 sludge floc matrix. *Appl. Microbiol. Biotechnol.* 43, 755-761.

- 421 Frostegård, Å., Tunlid, A., Bååth, E. (1991). Microbial biomass measured as total  
422 lipid phosphate in soils of different organic content. *J. Microbiol. Methods* 14, 151-  
423 163.
- 424 Judd, S.J. (2006). *The MBR book: Principles and applications in water and*  
425 *wastewater Treatment*. Elsevier Science, Amsterdam.
- 426 Kim, P.H.-S., Symons J.M. (1991). Using anion exchange resins to remove THM  
427 precursors. *J. Am. Water Works Assoc.* 83, 61-68.
- 428 Lapidou, C.S., Rittmann, B.E. (2002). A unified theory for extracellular polymeric  
429 substances, soluble microbial products, and active and inert biomass. *Water Res.* 36,  
430 2711-2720.
- 431 McAdam, E.J., Judd, S.J., Cartmell, E., Jefferson, B. (2007). Influence of substrate on  
432 fouling in anoxic immersed membrane bioreactors. *Water Res.* 41, 3859-3867.
- 433 McAdam, E.J., Judd, S.J. (2008). Biological treatment of ion-exchange brine  
434 regenerant for re-use: A review. *Sep. Purif. Technol.* 62, 264-272.
- 435 Petrovic, U., Gunde-Cimerman, N., Plemenitas, A. (1999). Salt stress affects sterol  
436 biosynthesis in the halophilic black yeast *Hortaea werneckii*. *FEMS Microbiol. Lett.*  
437 180, 325-330.
- 438 Peyton, B.M., Mormile, M.R., Peterson, J.N. (2001). Nitrate reduction with  
439 *Halomonas Campisalis*: Kinetics of denitrification at pH9 and 12.5% NaCl. *Water*  
440 *Res.* 35, 4237-4242.
- 441 Pflüger, K., Müller, V. (2004). Transport of compatible solutes in extremophiles. *J.*  
442 *Bioenerg. Biomembr.* 36, 17-24.
- 443 Reid, E., Liu, X., Judd, S.J. (2006). Effect of high salinity on activated sludge  
444 characteristics and membrane permeability in an immersed membrane bioreactor. *J.*  
445 *Membr. Sci.* 283, 164-171.

- 446 Russell, N.J. (1989). Adaptive modifications in membranes of halotolerant and  
447 halophilic microorganisms. *J. Bioenerg. Biomembr.* 21, 93-113.
- 448 Sutherland, I.W. (2001). Biofilm exopolysaccharides: a strong and sticky framework.  
449 *Microbiology* 147, 3-9.
- 450 Wilén, B.-M., Jin, B., Lant, P. (2003). The influence of key chemical constituents in  
451 activated sludge on surface and flocculating properties. *Water Res.* 37, 2127–2139.
- 452 Yakimov, M.M., Giuliano, L., Chernikova, T.N., Gentile, G., Abraham, W.-R.,  
453 Lünsdorf, H., Timmis, K.N., Golyshin, P.N. (2001). *Alcalilimnicola halodurans* gen.  
454 nov., sp. nov., an alkaliphilic, moderately halophilic and extremely halotolerant  
455 bacterium, isolated from sediments of soda depositing Lake Natron, East Africa Rift  
456 Valley. *Int. J. Syst. Evol. Microbiol.* 51, 2133-2143.
- 457 Yoshie, S., Ogawa, T., Makino, H., Hirosawa, H., Tsuneda, S., Hirata, A. (2006).  
458 Characteristics of bacteria showing high denitrification activity in saline wastewater.  
459 *Lett. Applied Microbiol.* 42, 277-283.
- 460 Zhang, X., Bishop, P.L., Kinkle, B.K. (1999). Comparison of extraction methods for  
461 quantifying extracellular polymers in biofilms. *Water Sci. Technol.* 39, 211–218.
- 462 Zhang, J., Chua, H.C., Zhou, J., Fane, A.G. (2006). Factors affecting the membrane  
463 performance in submerged membrane bioreactors. *J. Membr. Sci.* 284, 54-66.
- 464

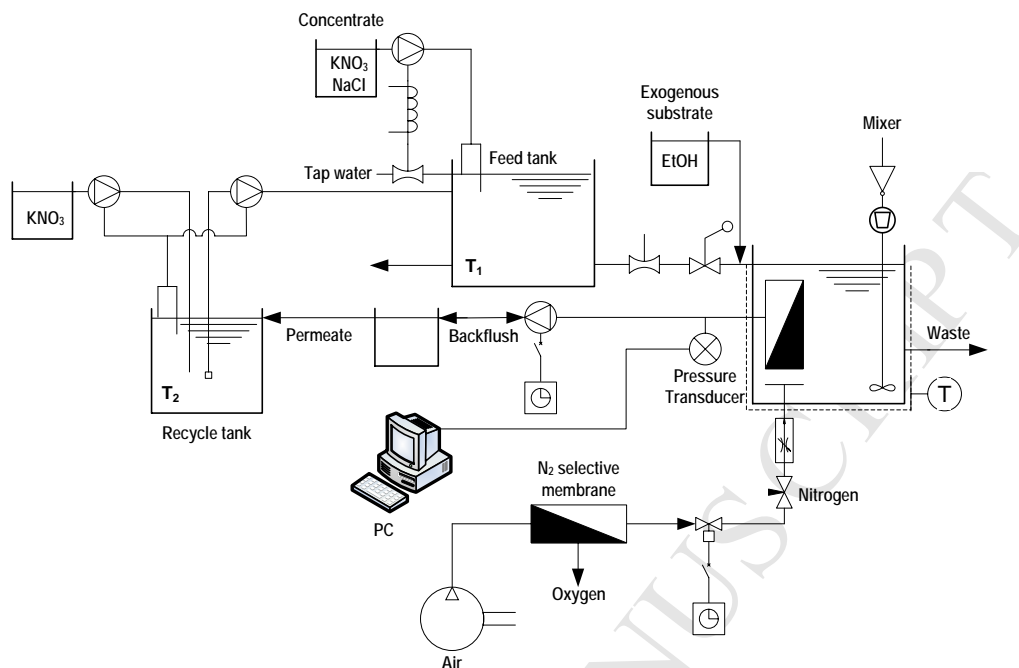


**Figure 1.** *Experimental set-up.*

**Figure 2.** *Optimising C:N ratio during steady state operation. Influent:  $500 \text{ mgNO}_3^- \cdot \text{N} \cdot \text{l}^{-1}$ ;  $50 \text{ gNaCl} \cdot \text{l}^{-1}$ .*

**Figure 3.** *Molecular weight SMP and permeate fractionation for protein and polysaccharide at steady state.*

**Figure 4.** *Impact of permeate recirculation to the main feed tank on dissolved organic carbon concentration (DOC) in the feed, permeate and SMP.*

**Figure 5.** *Critical flux analysis ( $J_c$ ) before, during and after permeate recirculation to the main feed tank. Specific gas demand per unit membrane area ( $\text{SGD}_m$ ),  $0.39 \text{ m}^3 \cdot \text{m}^{-2} \cdot \text{h}^{-1}$ .*

**Figure 6.** *Breakthrough curves observed from runs 2-6 using: (a) freshly produced brine; and (b) biologically treated brine. Influent concentration:  $\text{NO}_3^- \cdot \text{N}$   $22.6 \text{ mg} \cdot \text{l}^{-1}$ ;  $\text{SO}_4^{2-}$   $30 \text{ mg} \cdot \text{l}^{-1}$ ;  $\text{Cl}^-$   $115 \text{ mg} \cdot \text{l}^{-1}$  and  $\text{HCO}_3^-$   $150 \text{ mg} \cdot \text{l}^{-1}$ .*

**Figure 7.** *Adsorption of regenerant organics (protein, polysaccharide and DOC) by anion exchange resin.*

**Figure 8.** *Impact of salt upshock on biologically derived organics measured in the SMP.*

**Figure 9.** Critical flux analysis ( $J_c$ ) before and after each increase in salt concentration. Specific gas demand per unit membrane area ( $SGD_m$ ),  $0.39 \text{ m}^3 \cdot \text{m}^{-2} \cdot \text{h}^{-1}$ .

**Figure 10.** First and second principal components (PCs) derived from phospholipid fatty-acid profiles originating from biomass samples at the three salinities. Mean and standard deviation plotted. Percentage variation accounted for by PC shown in parenthesis on each axis.

**Table 1.** Treatment performance during salt spiking.

NaCl (g.L <sup>-1</sup> )	Recovery Time	C:N	NO <sub>3</sub> <sup>-</sup> -N	Ethanol <sup>a</sup>
			Repl. (%)	(mg.L <sup>-1</sup> )
50	N/a	0.92	99.7	4.1
75	24 h	0.87	60.1	75.1
	7 d	0.91	58.6	113
100	24 h	0.97	73.6	176.7
	7 d	0.99	73.3	209
50 <sup>b</sup>	24 h	0.94	98.4	10.7

<sup>a</sup>Permeate concentration. <sup>b</sup>Salt downshock.

**Table 2.** Major constituents of PLFA analysis (%).

	NaCl Concentration		
	50	75	100
C16:0	13.87	13.04	13.62
C16:1	24.95	27.12	26.06
C17:0	2.45	1.76	1.73
Exhibit 1 <sup>a</sup>	48.9	50.47	51.2
C19:0cy	7.07	5.24	4.77
Total (%)	97.2	97.6	97.4
Cyc/ cis	0.145	0.110	0.093

<sup>a</sup>Exhibit 1 – Comprises C18:0 and C18:1ω9c

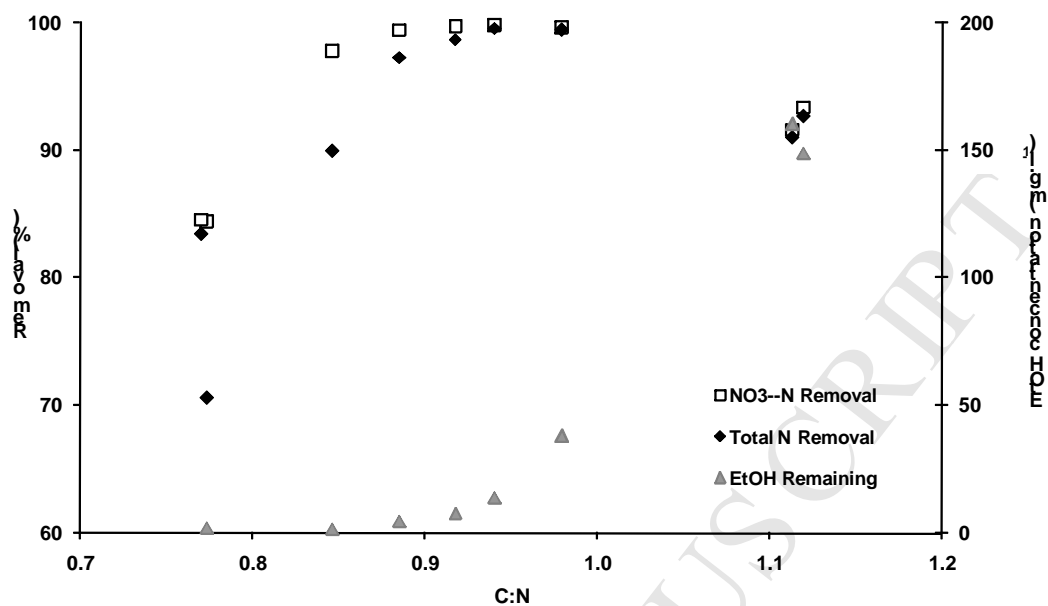


**Figure 2.** Optimising C:N ratio during steady state operation. Influent: 500 mgNO<sub>3</sub><sup>-</sup>-N.L<sup>-1</sup>, 50 gNaCl.L<sup>-1</sup>.

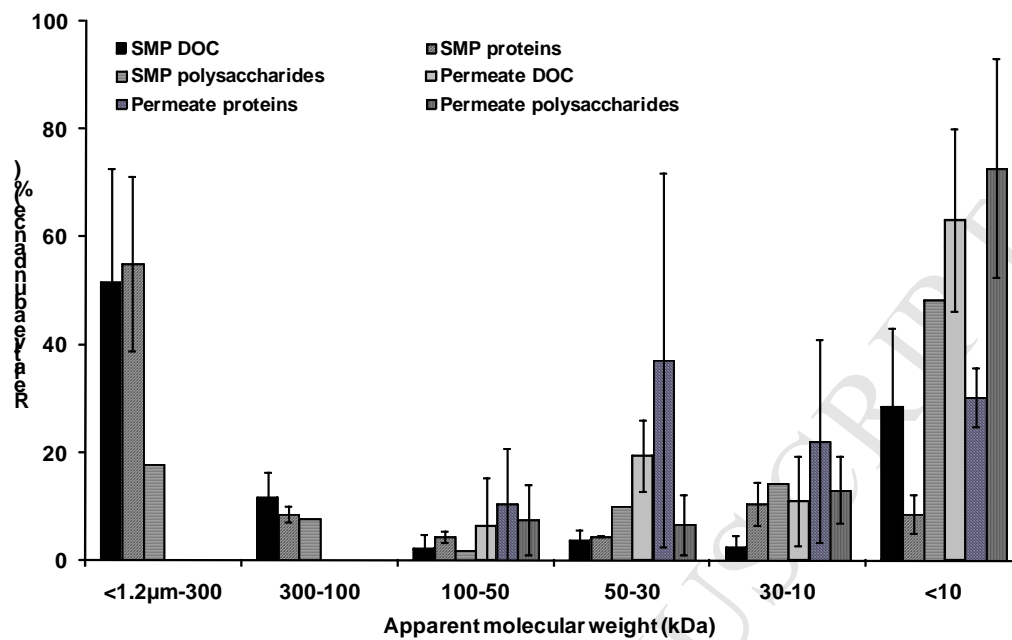


**Figure 3.** Serial fractionation of the SMP and permeate at steady state.



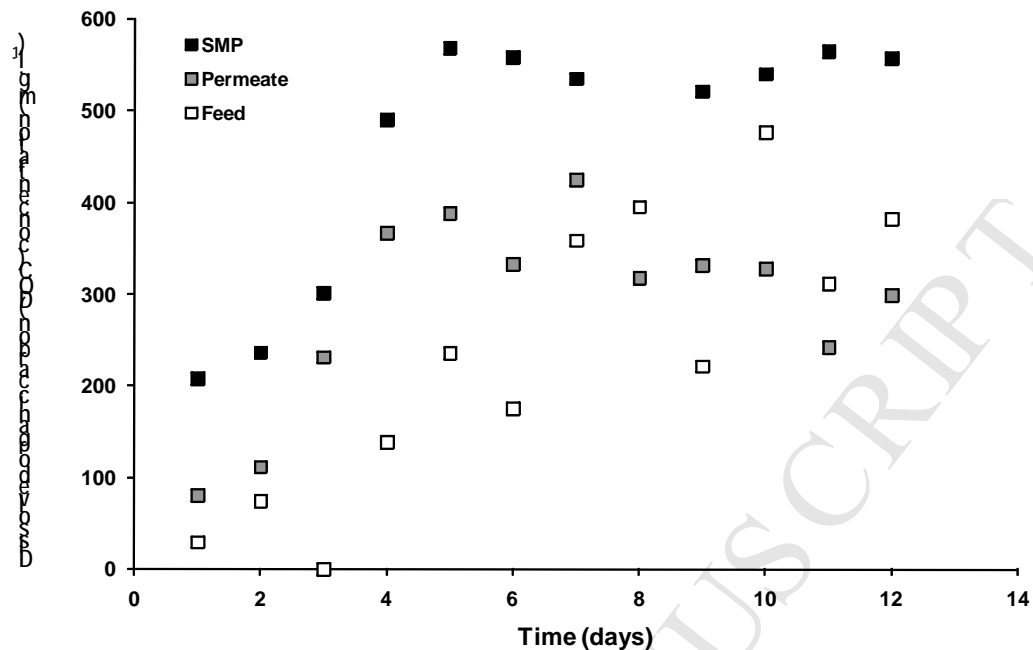


**Figure 4.** Impact of permeate recirculation to the main feed tank on dissolved organic carbon concentration (DOC) of the feed, permeate and SMP. Mean and standard deviation plotted. Percentage variation accounted for by PC shown in parenthesis on each axis.

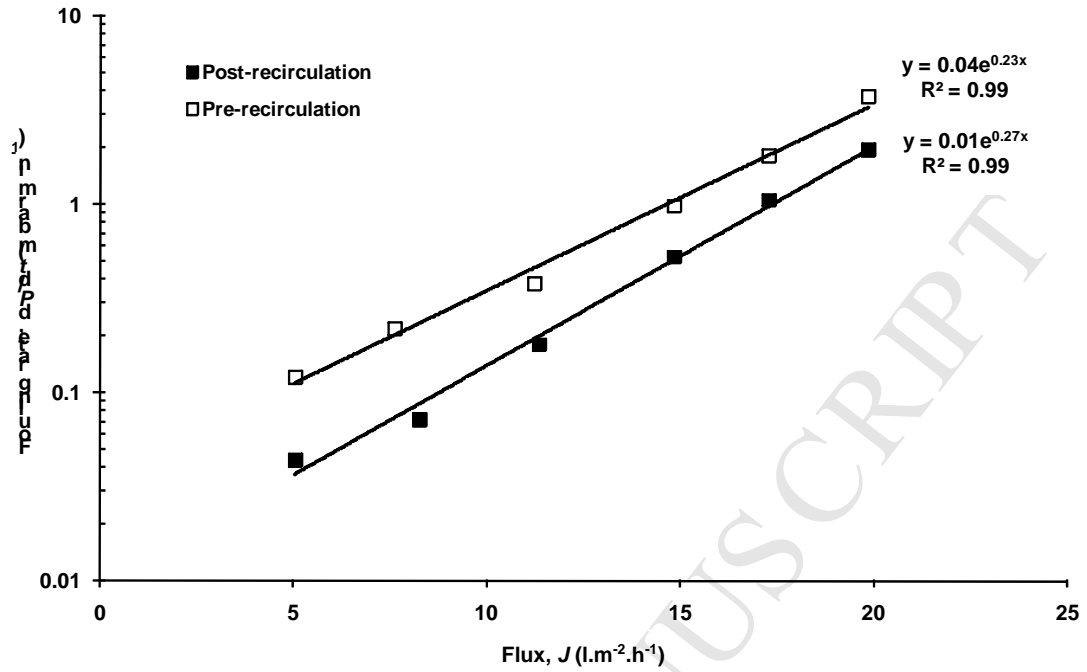
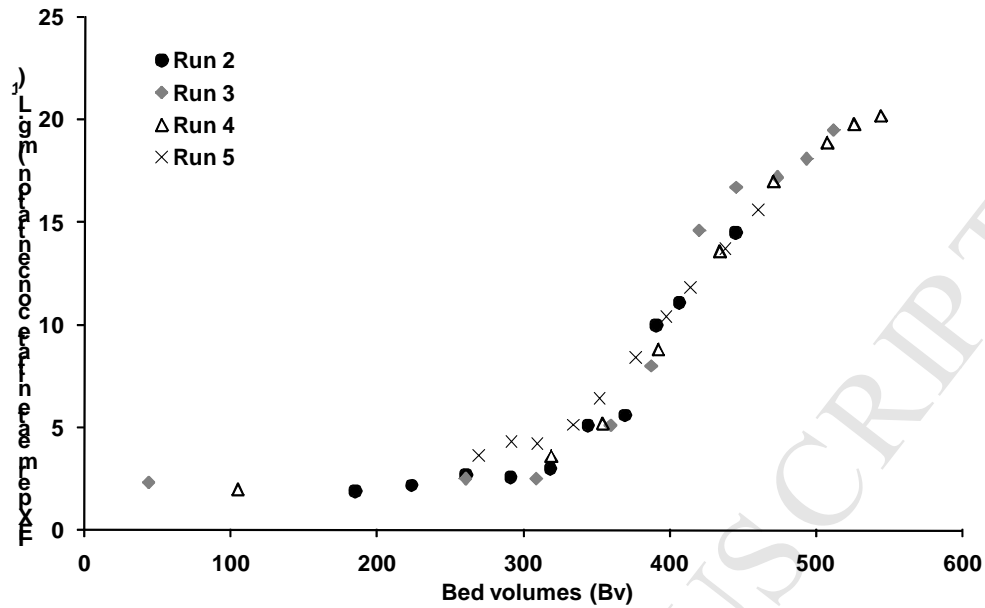
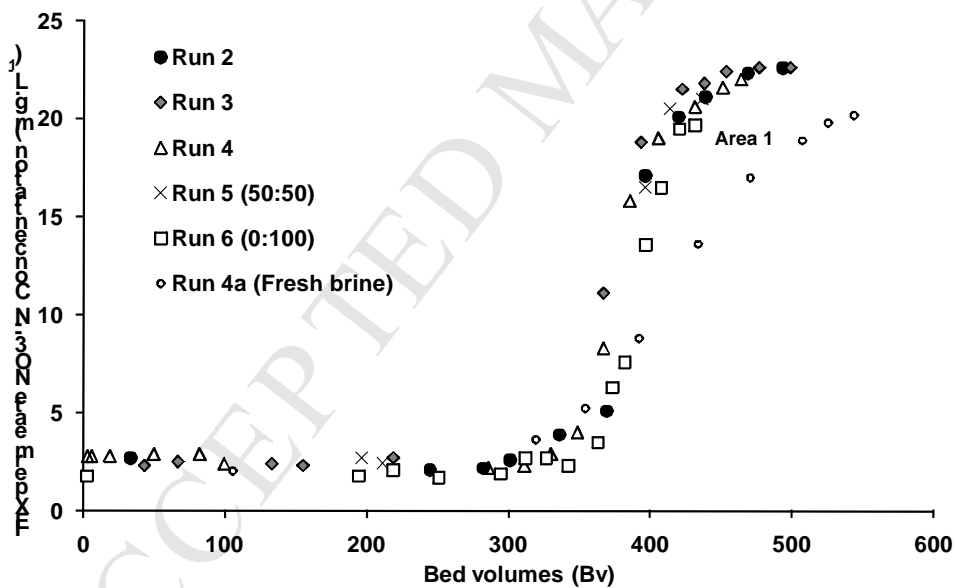


**Figure 5.** Critical flux analysis ( $J_c$ ) before, during and after permeate recirculation to the main feed tank.  $SGD_m 0.39 \text{ m}^3.\text{m}^{-2}.\text{h}^{-1}$ .



(a)



(b)

**Figure 6.** Breakthrough curves observed from runs 2-6 using: (a) freshly produced brine; and (b) biologically treated brine. Influent concentration:  $\text{NO}_3^-$ -N  $22.6 \text{ mg.L}^{-1}$ ;  $\text{SO}_4^{2-}$   $30 \text{ mg.L}^{-1}$ ;  $\text{Cl}^-$   $115 \text{ mg.L}^{-1}$  and  $\text{HCO}_3^-$   $150 \text{ mg.L}^{-1}$ .

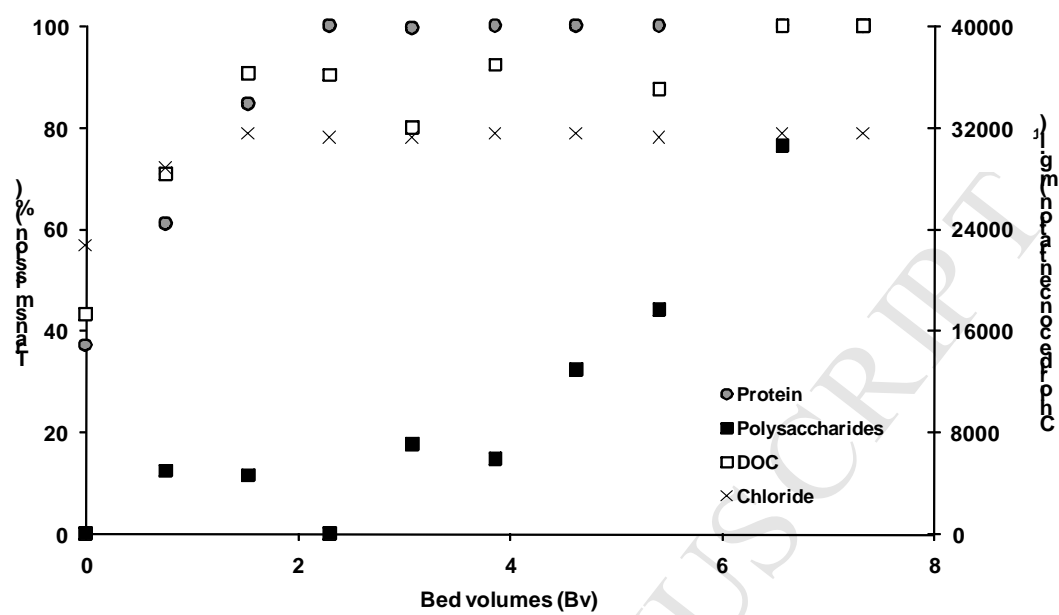


**Figure 7.** Adsorption of regenerant organics (protein, polysaccharide and DOC) by anion exchange resin.

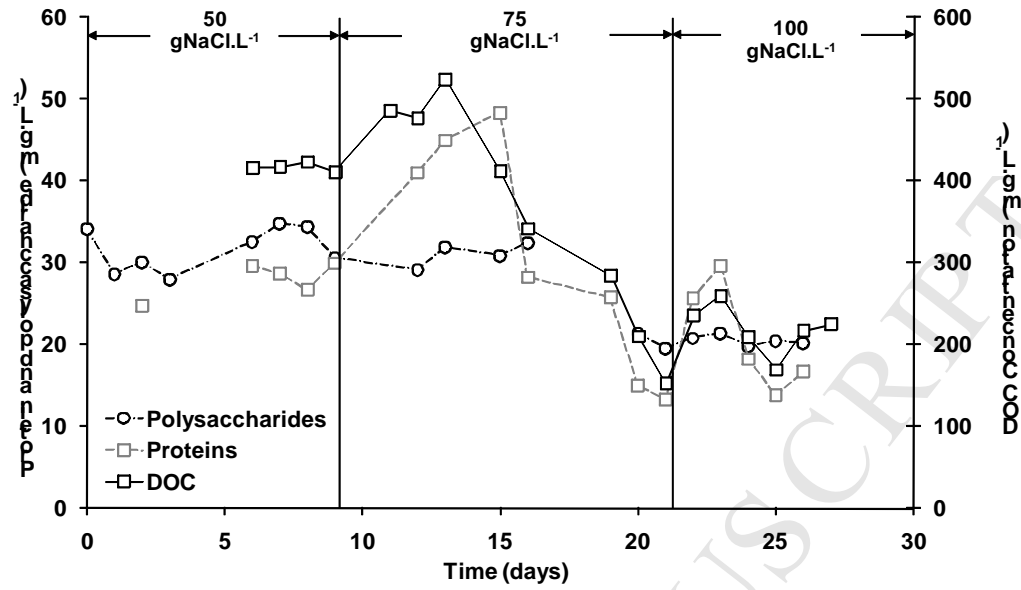


**Figure 8.** *Impact of salt upshock on biologically derived organics measured in the SMP.*

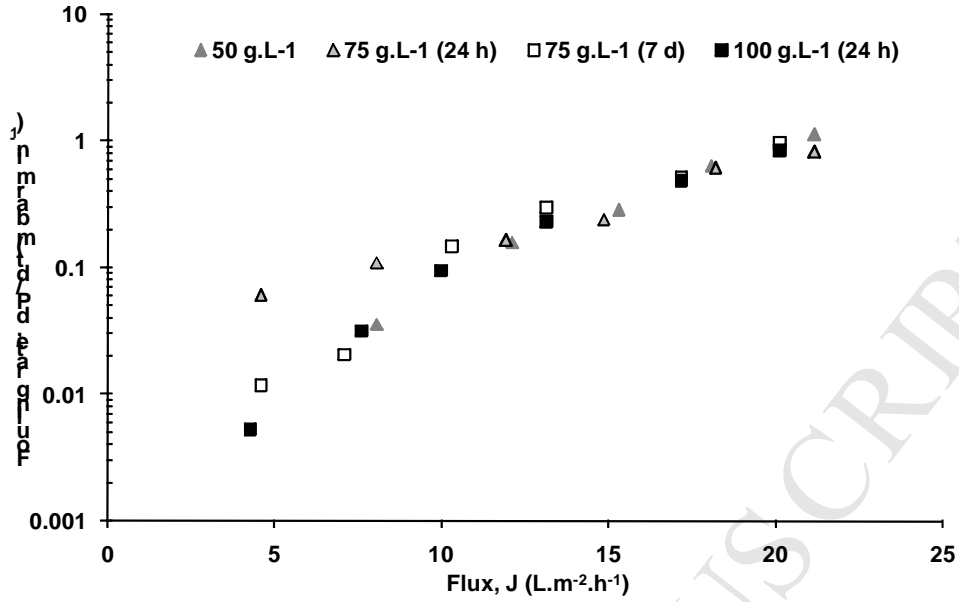


**Figure 9.** Critical flux analysis ( $J_c$ ) before and after each increase in salt concentration.  $SGD_m$   $0.39 \text{ m}^3 \cdot \text{m}^{-2} \cdot \text{h}^{-1}$ .

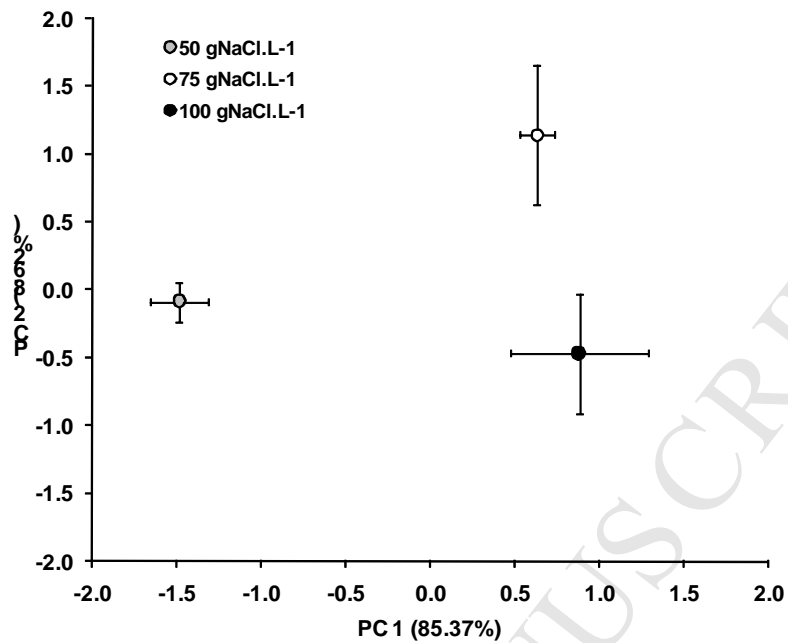


**Figure 10.** First and second principal components (PCs) derived from phospholipid fatty-acid profiles originating from biomass samples at the three salinities. Mean and standard deviation plotted. Percentage variation accounted for by PC shown in parenthesis on each axis.